



“Stump Horizon” in the Bílina Mine (Most Basin, Czech Republic) – GC–MS, optical and electron microscopy in identification of wood biological origin

Martina Havelcová^{a,*}, Ivana Sýkorová^a, Achim Bechtel^b, Karel Mach^c, Hana Trejtnarová^a, Margit Žaloudková^a, Petra Matysová^a, Jaroslav Blažek^a, Jana Boudová^d, Jakub Sakala^d

^a Institute of Rock Structure and Mechanics, Academy of Sciences of the Czech Republic, v.v.i., V Holešovičkách 41182 09 Prague, Czech Republic

^b University of Leoben, Applied Geosciences & Geophysics, Peter-Tunner-Str. 5, A-8700 Leoben, Austria

^c Severočeské doly a.s., Doly Bílina, ul. 5. května 213, 418 29, Bílina, Czech Republic

^d Charles University in Prague, Faculty of Science, Institute of Geology and Palaeontology, Albertov 6, 128 43 Praha, Czech Republic

ARTICLE INFO

Article history:

Received 28 May 2012

Received in revised form 5 September 2012

Accepted 17 September 2012

Available online 25 September 2012

Keywords:

Xylite
Gelification
Biomarkers
Cupressaceae s.l.
Lignite
Miocene
Most Basin

ABSTRACT

Numerous coalified tree stumps remained preserved *in-situ* in the so-called “Stump Horizon” (the palaeontologic horizon No. 31), which represents clayey overburden of the main coal seam in the Bílina open cast mine in the Most Basin (Czech Republic). The petrological and chemical composition, palaeobotanical origin and preservation of 24 selected tree stumps were studied by optical and scanning electron microscopy and gas chromatography–mass spectrometry (GC–MS). Composition of the fossil wood is dominated by ulminite, particularly texto-ulminite B. Textinite forms up to 38 vol.% in the decomposed tree stumps. Corpohuminite dominates in bark and root tissues. Partly gelified and deformed woody tissues contain both corpohuminite and resinite fillings. Random reflectance of ulminite ranges from 0.33% to 0.39% and carbon content from 49 wt.% to 78 wt.%. Samples represent pure woody material with small admixtures of clay minerals, siderite, and very rare pyrite. Observations by scanning electron microscopy revealed various levels of deformed secondary xylem with more or less swollen cell walls, conspicuous tracheids, uniseriate rays of a different height, and round or cylinder-like resin or corpohuminite bodies. According to our results and other published data the wood might belong to *Glyptostroboxylon* and *Taxodioxylon* genera that are supposed to belong to *Glyptostrobus* and *Quasisequoia* plants respectively, representatives of the coniferous family Cupressaceae. The biomarker composition in the extracts of the fossil wood includes sesquiterpenoids (α -cedrane, drimane, eudesmane), diterpenoids (abietane, fichtelite, 16 α (H)-phylocladane) and their degraded compounds. The terpenoids are derived from precursors produced by the source plants and microorganisms. The terpenoid signatures support a relationship to the Cupressaceae family with input of microbial species. These characteristics were identical for all studied samples. Significant variations have been observed in sesquiterpenoid α -cedrane and diterpenoid 16 α (H)-phylocladane contents.

© 2012 Elsevier B.V. All rights reserved.

1. Introduction

Fossil woods are common constituents in sedimentary sequences worldwide and in the calcified, silicified or charred forms may exhibit a high degree of anatomical preservation. These materials represent an important archive of data for palaeoenvironmental reconstructions (Falcon-Lang, 2005; Figueiral et al., 1999; Jeong et al., 2009; Kunzmann et al., 2009; Teodoridis and Sakala, 2008; Visscher and Jagels, 2003; Witke et al., 2004; Yoon and Kim, 2008). Part of fossil wood forms mummified, humified and gelified wood with variable preserved cell tissue structure, which is problematic for palaeoecological studies (Figueiral et al., 1999; Sweeney et al., 2009). Relationship between gelification, coalification, microscopic appearance, and chemical composition and structure of wood has been described in many Tertiary

deposits, e.g., Victorian brown coal in Australia (Russel, 1984; Russel and Barron, 1984), Greece (Kalaitzidis et al., 2004), Poland (Drobnik and Mastalerz, 2006; Wagner, 1982), Canada (Sykes, 1994), and Hungary (Erdei et al., 2009; Hámor-Vidó et al., 2010). Coalified fossil woods are usually deformed by the hydrostatic pressure of buried sediments, whereas petrified cherts and siderite coal balls preserve the original geometry of fossilized plant tissues (Hámor-Vidó et al., 2010; Sweeney et al., 2009).

The deformation and homogenization of gelified cellular structure caused a problem in the study of wood anatomy and identification of botanical affinity of coalified fossil wood. An effective technique in identification of plant tissue types is the old technique of etching of polished surfaces with oxidizing agents as summarized by Stach et al. (1982) and Taylor et al. (1998). Vassio et al. (2008) or Gryc and Sakala (2010) used a method based on boiling of wood in water for several hours to soften it before preparation of thin sections for a microscopic study in transmitted light. Figueiral et al. (2002) used

* Corresponding author. Tel.: +420 266009283.

E-mail address: havelcova@irmsm.cas.cz (M. Havelcová).

laboratory charring of wood specimens followed by taxonomy identification by reflected light microscopy. The botanical affiliation of the fossil wood can be also determined based on the molecular composition of terpenoid hydrocarbons. Chemotaxonomical classification of fossil fragments is based on majority of terpenoids in agreement with pollen elements representing a forest swamp environment (Bechtel et al., 2007; Otto and Wilde, 2001; Stefanova et al., 2005; Zdravkov et al., 2011).

Previous research on coalified fossil wood has largely focused on the chemical and petrographical characterization of organic matter, its deformation, degradation, mineralization, and determination of botanical affiliation of woody materials from the fossil forests or tree stumps and trunks in coal seams (Bechtel et al., 2007, 2008; Hámor-Vidó et al., 2010; Sweeney et al., 2009; Sykes, 1994; Vassio et al., 2008).

This study has investigated petrological and chemical properties of selected coalified woods from the Miocene “Stump Horizon” in the Bílina open pit mine in the Most Basin. The attention was also paid to determination of the palaeobotanical origin and the way of preservation of selected tree stumps using optical and scanning electron microscopy (SEM) and gas chromatography–mass spectrometry (GC–MS) analysis of extracts.

2. Geological settings

Since the opening of the Bílina open cast mine (exploiting 9 million tonnes of brown coal per year) on the top of coal seam 2–5 m thick uniform layer of clay rich in coalified remains of *in-situ* growing trees has been documented. Numerous coalified tree stumps remained preserved *in-situ* in clay overburden up to 5 m thickness of the main coal seam in the Bílina open cast mine in the Most Basin, Czech Republic (Fig. 1). This so called “Stump Horizon” is a clastic time equivalent of the lower half of the upper bench of the main coal seam within the Holešice Member of the Miocene age (Fig. 2). It consists of 2–4 distinguished horizons of stumps. Laterally this layer gradually turns to a clear coal bench. Vertically it gradually changes into prodeltaic laminated clays and a 100 m thick lacustrine deltaic system. This layer covers an area

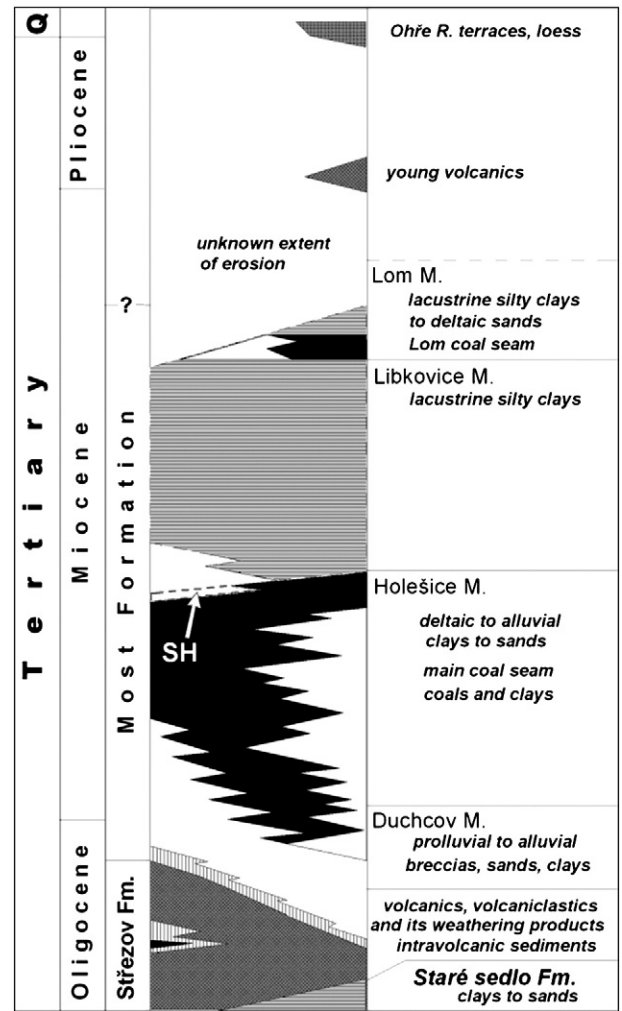


Fig. 2. Stratigraphy of the Most Basin fill. SH – “Stump Horizon” in the Bílina open pit mine.

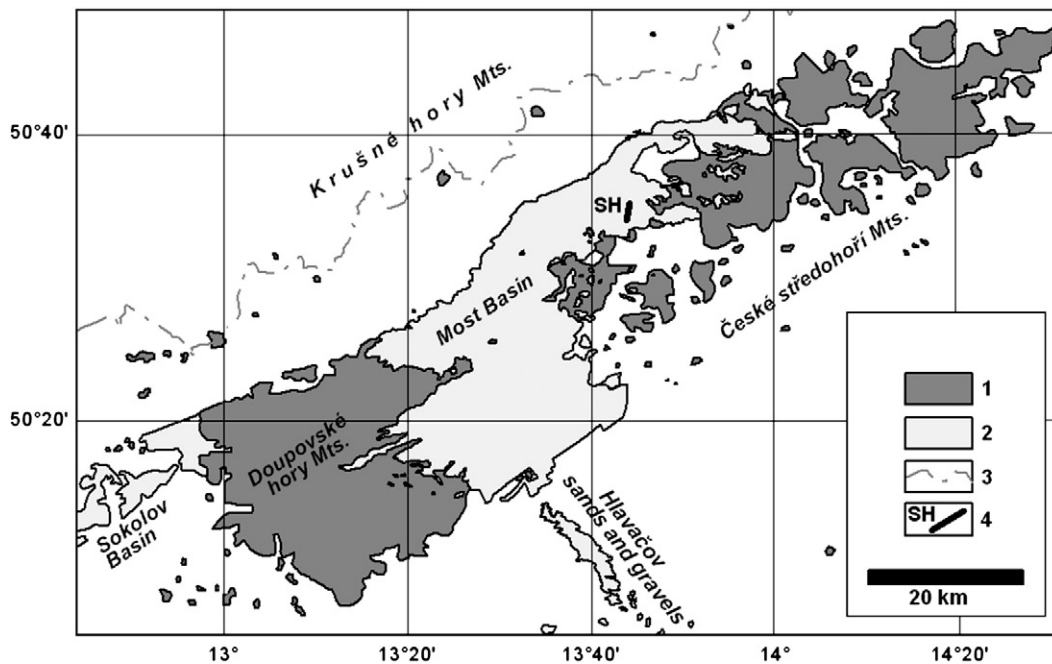


Fig. 1. Sketch map of the Most Basin. 1 – Oligocene volcanics (alkalic basalts, trachytes, phonolites) and its volcanoclastic equivalents; 2 – Lower Miocene sedimentary fill of the Most Basin (sands, clays, coal seam); 3 – state border; 4 – SH - area of “Stump horizon” sampling.



Fig. 3. Position of a stump in the layer of clay.



Fig. 4. Location of the studied subsamples in the one stump.

of 10×1 km. It is interpreted as an early stage of the Miocene development of the Břilina (river) delta. Grey clay sediment conserving coalified stumps and filling hollow trunks is thinly layered by organic detritus containing prevalently coniferous needles, twigs and cones, leaves and root systems of paludal grasses, ferns, floating ferns, *Calamus palmetto*, and several types of angiosperm swampy elements. Among the coniferous macrofossils, the most abundant are remains of leaves and cones of *Glyptostrobus europaeus* (Brongniart) Unger and *Quasisequoia couttsiae* (Heer) Kunzmann (Kvaček, 1998; Teodoridis and Sakala, 2008).

Most of the tree stumps are more or less hollow, around 1 to 5 m high and up to 2 m in diameter. They are exposed in three to four altitudinal subhorizons, mostly in upright position, some of them leaned to the clastic input source line (channel). They are accompanied by abundant siderite concretions.

3. Samples and methods

3.1. Samples

Coalified fossil wood samples from 23 selected stumps were collected (Fig. 3) and analysed. From one of the stumps, 9 sub-samples were taken which represent 8 selected parts of the trunk and roots and one sample of the woody detritus from the surrounding sediment (Fig. 4). Overview of the studied samples, dimensions of the found parts of trees, their characterization, and localization of the samples is given in Table 1.

From characteristic pieces of dull, brown to black-brown fossil wood (xylite), pieces oriented along the transverse, radial and tangential cuts were thoroughly selected and treated. Subsequently, polished sections for optical microscopy and samples for scanning electron microscopy were prepared from them. On polished sections with transverse and radial cuts, detailed exploration of morphology of

Table 1
Overview of the studied fossil wood samples with their general characteristics.

Number of the sample	Tree diameter (m)	Height (m)	Short description of stump	Deformation	Sample
S1–S9	1	1.2	Massive, in the upper part selectively to ribbon-form remnants digested	Medium	8 samples from the whole stump + 1 clay (see Fig. 4)
P1	1.1	1.5	Selectively to ribbon-form remnants digested and massive in the lower part	Medium	Middle part
P2	1.8	>2	Massive, almost without deformation	Low	Upper middle part
P3	1.4	>1	Hollow and deformed	Medium	North side with the lower deformation
P4	0.8	1.2	Selectively to ribbon-form remnants digested	Medium	Middle part
P5	1.2–1.8	1.5	Hollow like bowl-formed and splayed, selectively to ribbon-form remnants digested	medium–strong	Middle part of the “bowl”
P6	1.5	0.7	Strongly deformed lower part	Strong	North side
P7	0.5	0.6	Massive	Medium	Upper part
P8	0.45	0.9	Massive, tip tilted slightly, in the upper partially selectively to ribbon-form remnants digested	Low	North side
P9	0.65	0.6	Massive	Low	North upper part
P10	1.8	1.8	Strongly deformed, in upper part hollow like bowl-formed, in lower massive	Strong	middle part
P11	1	>1	Massive, tilted slightly, selectively sideritized	Low	Upper middle part + pelocarbonate
P12	1	>0.5	Strong deformed, lower part of the stump	Low	Middle part
P13	0.8	>0.5	Massive, tilted 60° to the south	Low	Middle part
P14	1	>0.5	Selectively to ribbon-form remnants digested, strong deformed, tilted 45° to the west, lower part of the stump	Low	Sampled from relatively low deformed part
P15	0.7	>0.5	Selectively to ribbon-form remnants digested, deformed	Medium	Middle part
P16	1.8	>1	Massive, partly deformed, selectively sideritized	Medium	From relatively low deformed part + pelocarbonate
P17	0.8	0.7	Selectively to ribbon-form remnants digested	Medium	North part
P18	1.8	1.3	Seemingly massive, upper part collapsed into the lower hollow digested part (tracheids oriented in various directions)	Strong	Central section of the upper part
P19	1.2	1	Seemingly massive, upper part collapsed into the lower hollow digested part (tracheids oriented in various directions)	Strong	Middle deformed part
P20	1.5	2.5	Massive, slightly tilted to the north, in upper part strongly deformed, in middle part undulating	Low–strong	Middle low deformed part
P21	1.8	>2	Massive, in upper part digested, tilted 45° to north	Medium	Middle part
P22	0.8	1.5	Massive, in upper part digested, tilted 45° to north	Low	Middle part
P23	<1	<1	Selectively to ribbon-form remnants digested	Low	North outer part

Table 2
Results of micropetrographic analysis of stumps P1–23.

Parametr	P1	P2	P3	P4	P5	P6	P7	P8	P9	P10	P11	P12	P13	P14	P15	P16	P17	P18	P19	P20	P21	P22	P23
Rr (%)	0.36	0.37	0.37	0.39	0.36	0.37	0.38	0.37	0.35	0.38	0.38	0.38	0.36	0.36	0.37	0.38	0.39	0.35	0.37	0.38	0.36	0.37	0.38
s	0.04	0.03	0.03	0.05	0.02	0.02	0.05	0.04	0.06	0.04	0.05	0.03	0.03	0.03	0.04	0.05	0.05	0.04	0.05	0.04	0.30	0.05	0.04
R_{TUA} (%)	0.25	0.00	0.00	0.00	0.24	0.23	0.25	0.00	0.00	0.00	0.00	0.00	0.00	0.00	0.23	0.23	0.24	0.23	0.24	0.00	0.00	0.00	0.00
Huminite (vol.%)	93.7	90.4	92.1	93.9	89.5	90.4	91.7	91.7	89.0	89.4	90.6	91.8	93.0	93.7	91.7	93.5	91.3	91.2	93.8	93.4	90.8	90.6	92.5
Textinite	26.1	6.4	20.3	13.3	15.8	18.9	6.4	14.7	6.1	15.8	5.3	26.3	9.2	2.3	28.4	37.3	5.9	2.9	2.0	9.3	3.2	5.5	5.0
T_A	1.5	0.0	0.0	0.0	0.8	0.0	0.0	0.0	0.0	0.5	0.0	0.3	0.0	0.0	0.5	0.8	0.0	0.0	0.0	0.0	0.0	0.0	0.0
T_B	25.0	6.4	20.3	13.3	15.0	18.9	6.4	14.7	6.1	15.3	5.3	26.0	9.2	2.3	27.9	36.5	5.9	2.9	2.0	9.3	3.2	5.5	5.0
Texto-ulminite	48.8	43.9	55.8	66.2	59.6	57.7	67.2	60.6	67.0	55.3	72.2	51.0	72.7	81.6	50.9	43.5	73.5	72.5	78.2	69.7	72.9	69.7	71.6
TU_A	0.5	0.0	0.0	0.0	1.3	1.5	2.7	0.0	0.0	0.0	0.0	0.0	0.0	0.0	0.8	0.9	0.7	3.3	1.4	0.0	0.0	0.0	0.0
TU_B	48.3	45.9	55.8	66.2	58.3	56.2	64.5	60.6	67.0	55.3	72.2	51.0	72.7	81.6	50.1	45.4	72.8	69.2	76.8	69.7	72.9	69.7	71.6
Eu-ulminite	4.8	22.6	5.8	3.7	3.3	1.5	5.6	2.0	5.7	5.2	2.2	0.0	0.0	0.0	0.0	0.0	0.0	2.1	2.0	2.5	1.9	2.7	4.2
Attrinite	0.0	0.0	0.0	0.0	0.0	0.0	0.0	0.0	0.0	0.0	0.0	0.0	0.0	0.0	0.0	0.0	0.0	0.0	0.0	0.0	0.0	0.0	0.0
Densinite	0.0	0.0	0.0	0.0	0.0	0.0	0.0	0.0	0.0	0.0	0.0	0.0	0.0	0.0	0.0	0.0	0.0	0.0	0.0	0.0	0.0	0.0	0.0
Corpohuminite	11.6	14.4	10.3	10.7	10.8	12.3	9.6	14.4	10.2	13.1	9.6	14.3	11.1	7.5	11.6	12.7	11.9	12.5	10.3	11.2	11.5	12.7	10.9
Gelinite	2.4	1.1	0.0	0.0	0.0	0.0	2.9	0.0	0.0	0.0	1.3	0.2	0.0	2.3	0.8	0.0	0.0	1.7	1.3	0.7	1.3	0.0	0.8
Liptinite (vol.%)	5.1	7.1	4.9	5.0	6.6	6.3	5.8	6.5	5.7	6.4	5.6	5.1	5.9	3.8	6.2	5.5	7.5	4.7	4.4	5.4	5.2	6.6	5.0
Sporinite	0.0	0.0	0.0	0.0	0.0	0.0	0.0	0.0	0.0	0.0	0.0	0.0	0.0	0.0	0.0	0.0	0.0	0.0	0.0	0.0	0.0	0.0	0.0
Cutinite	0.0	0.0	0.0	0.0	0.0	0.0	0.0	0.0	0.0	0.0	0.0	0.0	0.0	0.0	0.0	0.0	0.0	0.0	0.0	0.0	0.0	0.0	0.0
Resinite	5.1	7.1	4.9	5.0	6.6	6.3	5.8	6.5	5.7	6.4	5.6	5.0	5.9	3.8	6.2	5.5	7.5	4.7	4.4	5.4	5.2	6.6	5.0
Liptodetrinite	0.0	0.0	0.0	0.0	0.0	0.0	0.0	0.0	0.0	0.0	0.0	0.0	0.0	0.0	0.0	0.0	0.0	0.0	0.0	0.0	0.0	0.0	0.0
Inertinite (vol.%)	0.0	2.0	0.6	0.0	2.0	0.6	0.0	0.0	0.0	0.0	0.8	0.0	0.0	0.6	0.0	0.0							
Fusinite	0.0	0.0	0.0	0.0	0.0	0.0	0.0	0.0	0.0	0.0	0.0	0.0	0.0	0.0	0.0	0.0	0.0	0.0	0.0	0.0	0.0	0.0	0.0
Funginite	0.0	2.0	0.6	0.0	0.0	0.0	0.0	0.0	0.0	0.0	0.0	2.0	0.6	0.0	0.0	0.0	0.0	0.8	0.0	0.0	0.6	0.0	0.0
Minerals (vol.%)	1.2	0.5	2.4	1.1	3.9	3.3	2.5	1.8	5.3	4.2	3.8	1.1	1.3	2.5	2.1	1.0	1.2	3.3	1.8	1.2	3.4	2.8	2.5
Clays	1.2	0.5	1.5	0.5	3.2	2.6	2.3	1.5	4.8	1.5	3.2	0.7	1.0	1.5	1.9	0.6	0.7	1.9	1.2	1.1	1.6	0.9	1.7
Carbonates	0.0	0.0	0.9	0.5	0.0	0.7	0	0.2	0.3	2.1	0.5	0.3	0.0	1.0	0.0	0.4	0.0	1.4	0.6	0.0	1.8	1.9	0.6
Sulphides	0.0	0.0	0.0	0.1	0.7	0.0	0.2	0.1	0.2	0.1	0.0	0.0	0.0	0.0	0.0	0.0	0.5	0.0	0.0	0.0	0.0	0.0	0.2
Quartz	0.0	0.0	0.0	0.0	0.0	0.0	0.0	0.0	0.0	0.0	0.0	0.0	0.0	0.0	0.0	0.0	0.0	0.0	0.0	0.0	0.0	0.0	0.0
Other	0.0	0.0	0.0	0.0	0.0	0.0	0.0	0.0	0.0	0.5	0.1	0.1	0.3	0.0	0.2	0.0	0.0	0.0	0.0	0.1	0.0	0.0	0.0
GI (gelification index)	2.2	10.9	3.0	5.3	4.0	3.1	11.8	4.3	11.9	3.8	14.3	1.9	7.9	35.5	1.8	1.2	12.5	26.3	40.8	7.8	23.8	13.2	15.3

Significance of bold are main maceral groups.

Significance of italics are sub-maceral groups.

Table 3
Results of micropetrographic analysis of the stump samples S1–S9.

Parameter	S1	S2	S3	S4	S5	S6	S7	S8	S9
R _o (%)	0.36	0.34	0.35	0.34	0.36	0.35	0.36	0.37	0.33
S	0.03	0.03	0.03	0.02	0.02	0.02	0.03	0.03	0.04
R _{TUA} (%)	0.0	0.2	0.2	0.21	0.22	0.2	0.24	0.25	0.22
Huminite (vol. %)	79.1	83.5	90.3	91.9	90.3	90.1	90.5	87.3	23.0
Textinite	1.9	16.5	15.5	38.3	12.3	13.5	5.7	10.8	0.4
TA	0.3	0.8	1.5	1.9	1.1	1.4	0.9	1.6	0.3
TB	1.6	15.7	14.0	36.4	11.2	12.1	4.8	9.2	0.1
Texto-ulminite	41.7	38.8	52.2	33.2	53.4	61.4	70.4	54.6	10.3
T _{UA}	0.0	2.3	2.0	0.0	0.0	0.0	1.9	2.1	2.9
T _{UB}	41.7	36.5	50.2	33.2	53.4	61.4	68.5	52.5	7.4
Eu-ulminite	20.3	5.0	6.6	1.2	7.4	1.7	3.8	2.0	1.3
Attrinite	0.0	0.0	0.0	0.0	0.0	0.0	0.0	0.0	0.0
Densinite	0.0	0.0	0.0	0.0	0.0	0.0	0.0	0.0	2.1
Corpohuminite	14.4	21.3	15.5	19.2	17.2	13.5	10.6	19.9	8.0
Gelinite	0.8	1.9	0.5	0.0	0.0	0.0	0.0	0.0	0.9
Liptinite (vol. %)	5.9	7.7	6.2	7.4	6.0	6.5	5.7	8.7	11.9
Sporinite	0.0	0.0	0.0	0.0	0.0	0.0	0.0	0.0	1.7
Cutinite	0.0	0.0	0.0	0.0	0.0	0.0	0.0	0.0	0.4
Suberinite	0.3	0.9	0.0	0.0	0.0	0.2	0.4	0.0	0.5
Resinite	5.6	6.8	6.2	7.4	6.0	6.3	5.3	8.7	5.1
Exsudatinitite	0.0	0.0	0.0	0.0	0.0	0.0	0.0	0.0	0.0
Liptodetrinite	0.0	0.0	0.0	0.0	0.0	0.0	0.0	0.0	2.6
Inertinite (vol. %)	0.0	2.0	0.6	0.0	2.5	0.0	0.0	0.0	0.9
Fusinite	0.0	0.0	0.0	0.0	0.0	0.0	0.0	0.0	0.0
Funginite	0.0	2.0	0.6	0.0	2.5	0.0	0.0	0.0	0.9
Minerals (vol. %)	15.0	6.8	2.9	0.7	1.2	3.4	3.8	4.0	64.2
Clays	14.1	4.8	2.0	0.5	1.0	2.9	2.4	3.1	57.6
Carbonates, siderite	0.9	2.0	0.9	0.2	0.2	0.5	1.3	0.8	1.3
Sulphides	0.0	0.0	0.0	0.0	0.0	0.0	0.1	0.1	0.2
Quartz	0.0	0.0	0.0	0.0	0.0	0.0	0.0	0.0	0.0
Other	0.0	0.0	0.0	0.0	0.0	0.0	0.0	0.0	5.1
GI (gelification index)	33.0	2.8	3.8	1.0	4.9	4.7	9.5	5.2	33.0

Significance of bold are main maceral groups.

Significance of italics are sub-maceral groups.

cell tissues, gelification of cell walls, contraction fissures, resinite and corpohuminite forms, mineralization and weathering was performed. The rest of the sample was powdered (<3 mm), reduced in size by quartering, and powdered for optical microscopy (<1 mm) and chemical analyses (<0.2 mm).

3.2. Optical microscopy

Reflectance, as a parameter of coalification, was measured on homogeneous sites of ulminite B on grained polished sections according to ISO 7404 (2009) using a UMSP 30 Petro OPTON-ZEISS microscope, in monochromatic light ($\lambda = 546$ nm), with immersion objectives at 5 \times , 40 \times , and 400 \times magnifications. With the same apparatus, macerals were identified according to ISO 7404 and in accordance with the principles brought forward by Taylor et al. (1998), International Committee for Coal and Organic Petrology (ICCP) (2001), and Šýkorová et al. (2005). Determination of liptinite macerals was performed using the UMSP 30 Petro microscope with a fluorescence system. From the maceral composition, gelification index (GI) was calculated based on a principle of the proportion of gelified and ungelified huminite components, according to the equation proposed by von der Brellie and Wolf (1981):

$$GI = \frac{\text{Gelified telohuminite} + \text{Gelified detrohuminite} + \text{Gelinite}}{\text{Non gelified telohuminite} + \text{Non gelified detrohuminite}}$$

Attention was paid to discern their botanical characteristics with focus on earlywood and latewood tracheids, rays, and cross-fields, in accordance with scanning electron microscopy studies.

Tissue texture was studied on oriented polished sections using an OLYMPUS BX51 microscope for reflected light with a CRAIC system, dry objectives at 10 \times and 40 \times magnifications, and immersion objectives at 5 \times , 40 \times , and 100 \times magnifications.

3.3. Scanning electron microscopy

Scanning electron microscopy was used for detailed anatomical studies and documentation. Samples with well preserved and undistorted structure from selected pieces of wood were processed. The xylitic specimens were observed using a Quanta 450 scanning electron microscope (Institute of Rock Structure and Mechanics, Academy of Sciences of the Czech Republic), and were examined using a Jeol JSM-6380 LV scattered low-vacuum electron microscope at 15 kV (Institute of Geology and Palaeontology, Faculty of Science, Charles University in Prague). The anatomical description is in accordance with the IAWA Softwood terminology (IAWA Committee, 2004).

3.4. Chemical analysis

The elemental organic composition was determined using a CHNS/O microanalyser Flash FA 1112 Thermo Finnigan. For organic geochemistry analyses, wood fragments were powdered and Soxhlet-extracted with dichloromethane for 5 h. The solvent amount was reduced using a vacuum evaporator. The polar compounds were removed from the extracts using column chromatography on silica gel (Kieselgel 60, Merck). The aliphatic and aromatic hydrocarbon fractions were eluted by *n*-pentane and a mixture *n*-pentane:dichloromethane (1:1, v:v). The extracts were analyzed by GC-MS using a Thermo Scientific Trace Ultra DQ II instrument equipped with a capillary column with a fixed stationary phase DB 5 (30 m \times 0.25 mm \times 0.25 μ m film). The GC oven was heated from 35 $^{\circ}$ C (5 min) to 300 $^{\circ}$ C (10 min) at a rate of 4 $^{\circ}$ C/min. The analysis was carried out in the split mode (1:50). Helium was used as a carrier gas. Mass spectra were recorded at EI 70 eV from 40 to 500 amu in full scan mode. Identification of compounds was based on comparison of spectra with the National Institute of Standards and Technology (NIST) mass spectral library and data from literature (Philp, 1985).

4. Results

4.1. Petrographical characteristics of fossil wood

Reflectance and maceral analyses of 23 representative samples were carried out (Table 2). One stump was studied in detail (Table 3). Reflectance values range from 0.34% R_r to 0.39% R_r in trunk samples. The lowest value 0.33% R_r originates from ulminite of the woody fragments dispersed in carbonaceous clay surrounding the stump S. These values indicate a metatype lignite rank (ECE-UN, 1998). All wood samples dominantly consist of ulminite, particularly testo-ulminite B (Fig. 5). In some cases, dark ulminite A with reflectance lower than 0.25% R_{TUA} has been recognized in the cellular tissues. Textinite comprises up to 38.3 vol.% in the partly decayed tree stump S4 and 37.3 vol.% in P16. Dark textinite was observed in amounts less than 2 vol.% in samples S1–S9 and P1, P5, P10, P12, P15, and P16. Completely gelified cellular tissues occurred irregularly, eu-ulminite dominated in sample S1 and P2. A characteristic feature of the wood samples is the presence of corpohuminite bodies which infill cell lumens and comprise 7.5 vol.% to 21.3 vol.% of the wood. The corpohuminites are solid or finely porous, nonfluorescent, reflecting more than ulminite B, typically round to oval in transverse section, and elongated in oblique or longitudinal section. Resinite fillings of cellular and intercellular spaces range between 4.4 vol.% and 8.7 vol.% in S8 sample. Other liptinite macerals sporinite, cutinite, suberinite and liptodetrinite have been found in carbonaceous clayey rock PB9. Inertinite macerals are absent in the sample collection

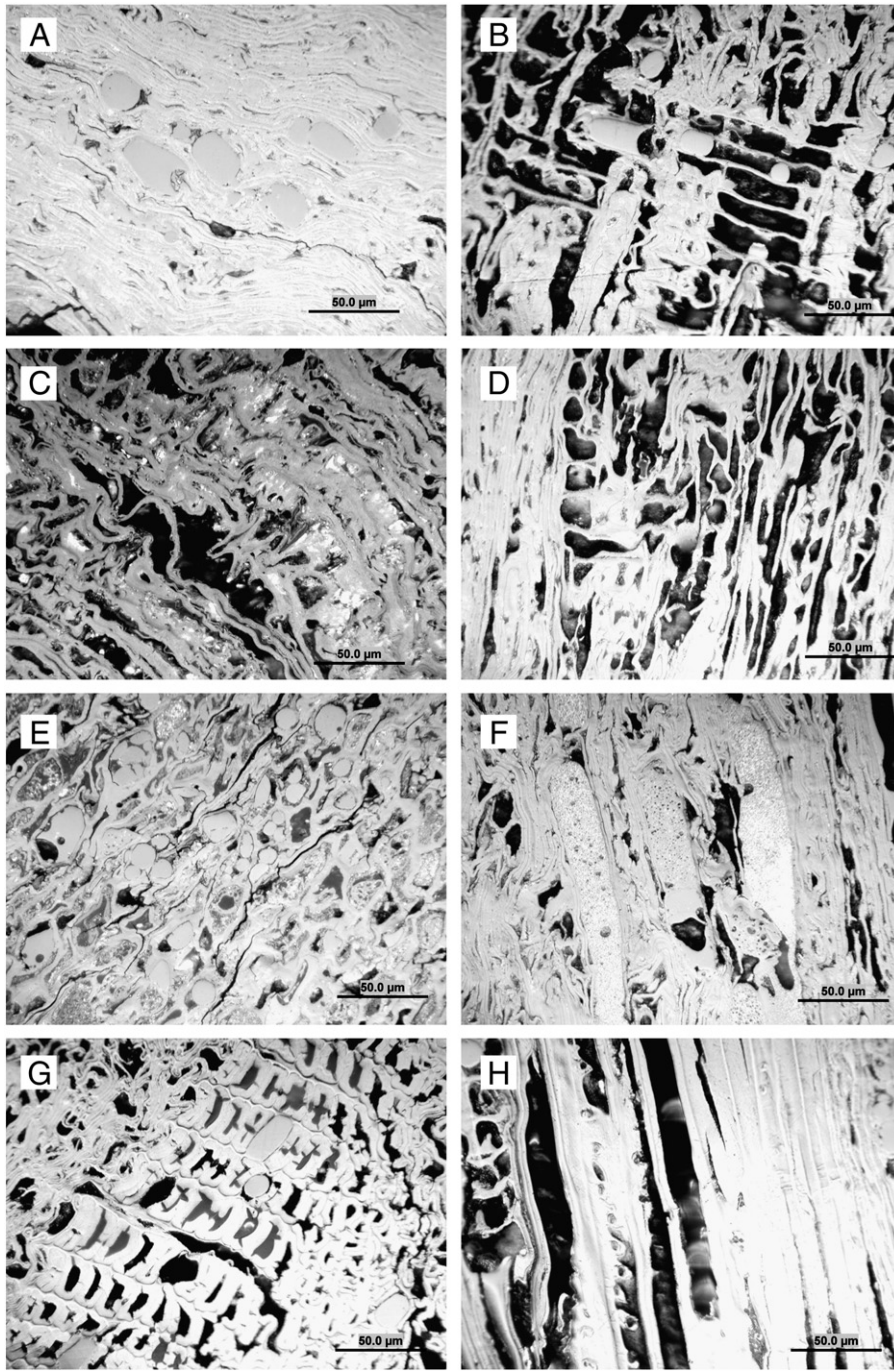


Fig. 5. Reflected light microphotographs of xylite samples showing the range of humotelinite structure preserved in wood tissues of coalified tree stumps. A. Ulminite and corpohuminite – deformed and gelified wood tissue of massive stump P1. B. Ulminite and corpohuminite – deformed and gelified wood tissue of massive stump P1. C. Textinitte B and ulminite B in cross-field in the partly gelified wood tissue in partly decayed stump P6, radial cut. D. Textinite A and transition to ulminite A which are impregnated by resinite, sample P5. E. Ulminite B and textinite in partly gelified wood tissue with deformed uniseriate rays (P9), tangential cut. F. Corpohuminite and resinite fillings in cell volumes of textinite and ulminite that represent partly swollen cell walls in partly decayed stump P15. G. Ulminite with transition to textinite and elongated fine porous corpohuminite in wood tissue of partly decayed stump P16. H. Textinite to ulminite with corpohuminite and resinite fillings of cell volumes in deformed and partly gelified tissue of earlywood and latewood, partly decayed stump P15, radial cut. I. Ulminite to textinite – poorly saved pits observed in fragment of tracheid. Partly decayed stump P23, radial cut.

with exception of funginite, which has been found in low concentrations in samples S2, S3, S7, S9, P2, P3, P12, P13, P18, and P21 (Tables 2 and 3). Samples represent clean woody material with small admixtures of clay minerals, massive bodies of siderite, and very rare framboidal and crystalline pyrite. The dominance of ulminite, lower contents of textinite and absence of humodetrinite correspond with values of the gelification index GI ranging between 1.0 and 40.8.

4.2. SEM characteristics

The SEM observation of prepared gelified wood fragments revealed various levels of deformed secondary xylem with more or less swollen cell walls with round and cylinder-like resin or corpohuminite bodies with various size (Fig. 6). In spite of an overall bad preservation of the anatomical features, two taxonomical units were identified –

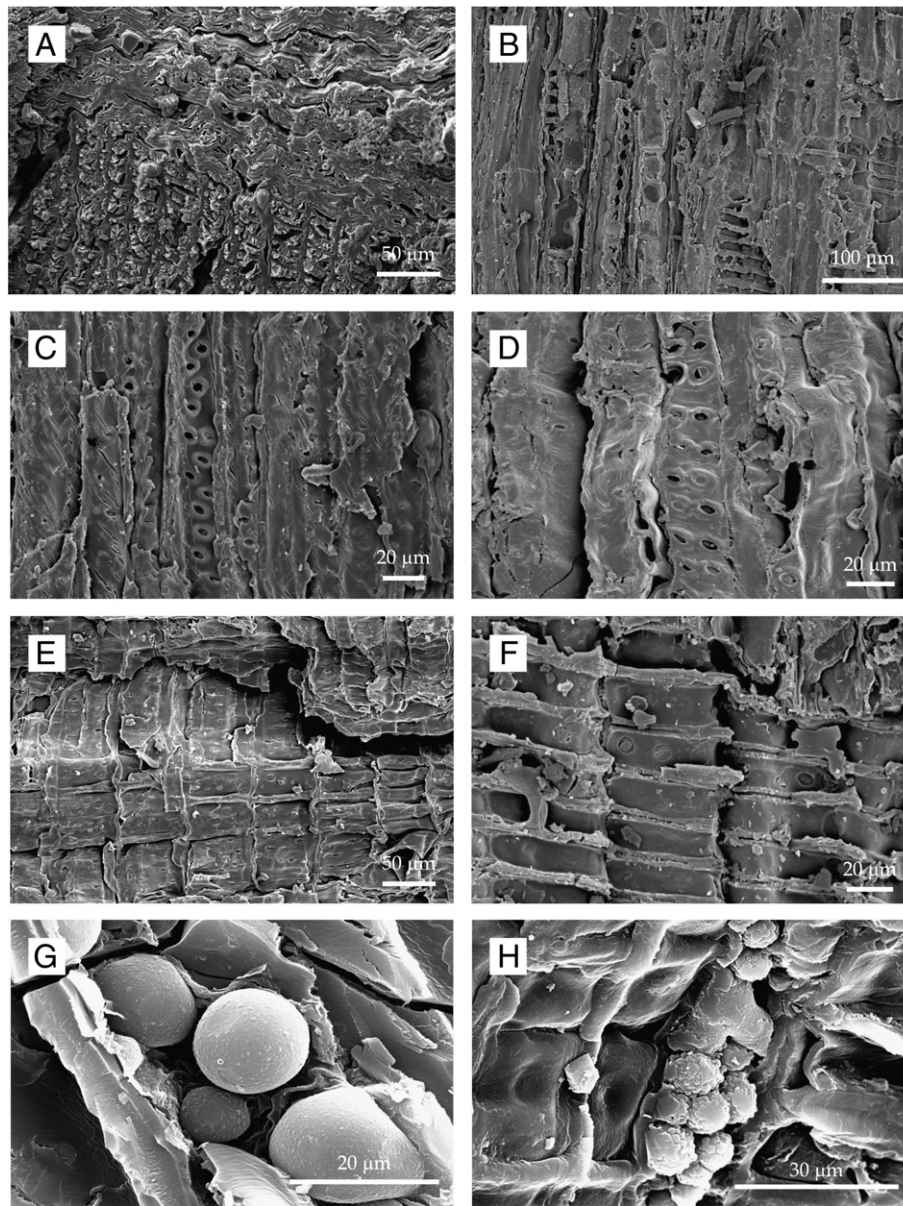


Fig. 6. SEM microphotographs of the microscopic structures of the wood tissues preserved in the coalified tree stumps. TS – transverse section; TLS – tangential longitudinal section; RLS – radial longitudinal section.

Glyptostroboxylon rudolphii:

- A TS, sample P15, general view with both early- and latewood, gelified and deformed.
 B TLS, sample P9, general tangential view with rays passing radial one demonstrating the deformed structure.
 C RLS, sample P8, uniseriate bordered pits in radial tracheid wall.
 D RLS, sample P18, regularly arranged biseriate pitting with crassulae.
 E RLS, sample S4, irregularly arranged “glyptostroboid” cross-field pits.

Taxodioxyton gypsaceum:

- F. RLS, sample P9, taxodioid cross-field pits in regular horizontal rows.
 G. RLS, sample P21, detail of spherical and irregular particles of resinite or corphuminite with relative smooth surface, which are discretely located in cell.
 H. RLS, Sample P21, detail of cauliflower-like particles of resinite fixed in cell walls.

Glyptostroboxylon rudolphii Dolezych & van der Burgh and *Taxodioxyton gypsaceum* (Goepfert) Krausel. The main criterion was type and regularity of both pitting in radial tracheid walls and cross-field pitting. These wood fragments have been interpreted in accordance with the previous study from the same area (Teodoridis and Sakala, 2008), i.e., *Glyptostroboxylon rudolphii* as wood of *Glyptostrobus europaeus*

and *Taxodioxyton gypsaceum* as wood of *Quasisequoia couttsiae*. Results of SEM studies correspond to the macrofossil record (Kvaček, 1998; Kvaček et al., 2004) of the layer studied.

The samples attributed to *Glyptostroboxylon rudolphii* (S4, S5, P1–P8, P10, P12, P14, P15, P17, and P20–P22) show growth rings, but transition between earlywood and latewood was not observed. Bordered pits

Table 4
Basic chemical characterization of the stump samples S1–S9 (a) and P1–P23 (b).

Sample	%W ^a	%A ^d	%C ^{daf}	%H ^{daf}	%N ^{daf}	%S ^{daf}	%SOM ^{daf}
a)							
S1	12.92	10.56	78.11	5.72	1.77	0.50	8.36
S2	20.76	9.12	70.10	5.25	1.58	0.50	15.94
S3	19.62	4.96	64.29	5.11	1.49	0.47	13.71
S4	19.25	1.37	74.40	5.71	1.40	0.42	14.97
S5	16.64	3.27	70.43	5.60	1.55	0.31	10.47
S6	20.40	1.60	73.06	5.62	1.64	0.42	13.32
S7	20.39	6.19	70.39	5.40	1.71	0.44	9.84
S8	28.71	2.34	70.41	5.47	1.32	0.36	19.51
S9	6.30	71.62	49.79	6.87	1.37	0.39	6.77
b)							
P1	14.20	2.36	71.45	4.98	1.95	0.02	8.44
P2	17.73	1.10	70.36	5.43	1.67	0.01	16.55
P3	15.65	2.66	71.14	5.02	1.83	0.03	9.56
P4	14.64	1.75	69.34	5.05	1.66	0.06	9.65
P5	14.75	1.10	69.53	5.17	1.67	0.03	14.80
P6	14.23	1.40	75.47	5.29	1.72	0.01	12.53
P7	12.28	14.49	71.77	5.27	1.61	0.01	9.64
P8	15.36	2.21	70.97	5.52	1.49	0.01	15.84
P9	13.37	6.16	73.56	5.24	1.66	0.20	11.15
P10	15.79	2.83	71.36	5.45	1.63	0.01	15.63
P11	11.47	5.14	69.59	5.05	0.91	0.39	1.11
P12	11.52	1.94	69.40	5.03	0.78	0.33	8.64
P13	11.23	1.69	63.68	5.04	0.78	0.38	12.67
P14	11.42	3.25	66.12	4.76	0.98	0.32	8.97
P15	10.15	2.39	69.56	5.19	0.65	0.38	10.72
P16	10.71	1.10	69.39	5.05	0.92	0.40	7.91
P17	10.30	1.65	70.56	5.33	0.81	0.40	11.82
P18	11.49	4.24	68.80	4.86	1.15	0.40	7.83
P19	10.66	2.31	68.93	4.94	1.05	0.36	6.54
P20	11.20	1.71	69.94	5.28	1.01	0.39	10.35
P21	10.02	4.10	68.36	5.15	0.77	0.40	10.18
P22	11.33	1.30	69.74	5.29	0.78	0.37	11.36
P23	13.21	3.26	67.79	4.90	1.02	0.37	8.46

%W – percent of moisture.

%A – ash yield.

%C – carbon content.

^aAnalytical sample.

^dDry.

^{daf}Dry ash free.

SOM Soluble organic matter.

are opposite, circular, in 1–2 irregular vertical rows in radial tracheid walls. Uniseriate rays composed solely of parenchyma cells without ray tracheids are up to 10 cells high with thin and smooth both horizontal and end (tangential) walls. The 1–3 mostly “glyptostroboid” (taxodioid with very narrow borders approaching almost pinoid) cross-field pits per field were irregularly arranged. The axial parenchyma was present often with the resin substance, the type of transverse end walls is unknown.

The samples attributed to *Taxodioxydon gypsaceum* (P9, P11, P13, P16, P18, P19, P23) have growth rings, but transition between earlywood and latewood was not observed. Bordered pits are opposite, circular, in 1–2 regular vertical rows in radial tracheid walls, and crassulae are often present. Uniseriate rays composed solely of parenchyma cells, without ray tracheids, up to 13 cells high with thin or slightly thickened and smooth both horizontal and end (tangential) walls. The 1–3 mostly taxodioid cross-field pits per field were arranged in regular horizontal rows. The axial parenchyma was present often with the resin substance, the type of transverse end walls is unknown.

4.3. Bulk chemical composition

Table 4 demonstrates that there are not significant differences in bulk chemical composition between samples from one trunk (S1–S9)

and samples from 23 stumps (P1–P23). Xylite samples are characterized by variable ash content (A^d) ranging between 1.30 wt.% and 10.56 wt.%. The highest ash content has been found in carbonaceous clay S9. Total sulphur content (%S^{daf}) varies up to 0.5 wt.%, and nitrogen content (%N^{daf}) up to 1.95 wt.% (Table 4). The carbon contents higher than 70 wt.% C^{daf} were determined in the samples S1–S8 from one stump and in the samples P1–P3, P6–P10, and P17. The highest carbon contents were found in the sample of gelified wood of the root S1 and in the sample of deformed wood P6 (Table 4).

4.4. Organic geochemistry

Examples of two typical chromatograms obtained for the samples P7 and P17 are shown in Fig. 7 (aliphatic fraction) and Fig. 8 (aromatic fraction) together with their detailed description. The total area given by the sum of the areas of all identified compounds was used as a reference for determining the relative content of an individual compound in the samples. The results for aliphatic and aromatic hydrocarbon fractions are shown in Tables 5 and 6, respectively (part a) – wood extracts S1–S9, part b) – wood extracts P1–P23).

5. Discussion

5.1. Gelification index, soluble organic matter, and carbon, nitrogen, sulphur and oxygen contents

The wood, bark and root samples are petrographically distinct, in terms of both maceral and tissue composition. They are dominated by gelified but structurally intact ulminite B with minor and variable proportions of textinite B and corpohuminite. The wood contains a low portion of varieties of textinite A and ulminite A with reflectance values lower than 0.25% (Table 2). The origin of both dark varieties of telohuminite can be ascertained from higher cellulose content, lower degree of humification and gelification, lower Eh and pH conditions, and from the type of vegetation and plant tissues (Russel, 1984; Russel and Barron, 1984; Stach et al., 1982; Sykes, 1994). Textinite and ulminite were studied from the anatomical point of view. Differences in petrological and chemical composition have been found among the wood samples from one stump as well as among the individual samples in the set of 23 stumps. Our results show large variability of GI values in the carbon rank range from 49 wt.% to 78 wt.% (Fig. 9).

According to Bechtel et al. (2002), sulphur content is associated with the degree of wood gelification. This does not appear in the studied samples. Fig. 10, Tables 2 and 3 show that all samples can be divided into three groups according to their sulphur contents. Sulphur content higher than 0.3 wt.% has been found in gelified wood with GI lower than 15 and in the group of samples with GI higher than 20. In samples with GI lower than 15, sulphur is present in trace amounts. It can be assumed that sulphur is represented primarily by organic sulphur. No pyrite was detected under optical microscopy in samples P6–P10 with very low sulphur and in the remaining samples it was rare. The stump samples (Fig. 10) were enriched with sulphur, which could be due to selective preservation of sulphur containing compounds (sulphur is largely bound to lignin and its derivatives) or may indicate anaerobic conditions during storage of wood, in the presence of anaerobic bacteria (Bechtel et al., 2002). The relative increase in sulphur may reflect preferential preservation and relative enrichment with sulphur as a result of removal of selected wood components, such as cellulose due to changing edaphic conditions Eh and pH (Drobnik and Mastalerz, 2006). Hatcher et al. (1981), Hatcher (1988), and Stout et al. (1989) found that cellulose is rapidly depleted and removed from organic material during early coalification via biological degradation whereas lignin is somewhat resistant to alteration. Results of the early stage coalification experiments show that both the cellulose and lignin components of the wood could be converted to vitrinite-like substances under pressure and temperature

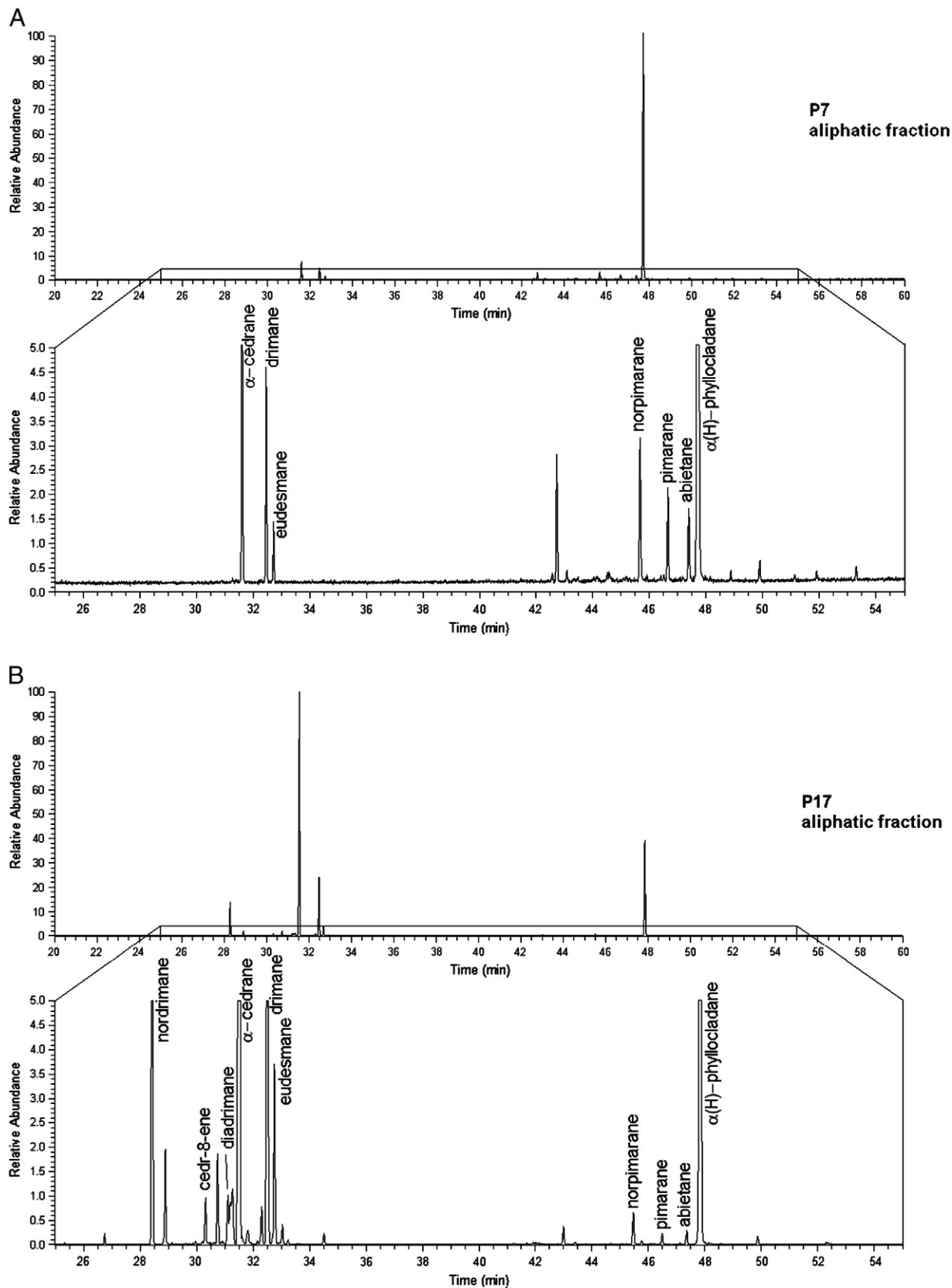


Fig. 7. Typical TIC (Total Ion Current) chromatograms of the aliphatic fraction of the sample extracts P7 (A) and P17 (B).

conditions without biochemical processes (Davis and Spackman, 1964; Rollins et al., 1991).

According to Bechtel et al. (2002) there is also a correlation between soluble organic matter (% SOM) and gelification degree (GI) of the

sample (the higher extractability is in non-gelified or low gelified wood fragments), and between nitrogen, sulphur and oxygen content (NSO) and gelification (GI) of the sample (the larger GI, the higher NSO). We have not found such dependence. In accordance with

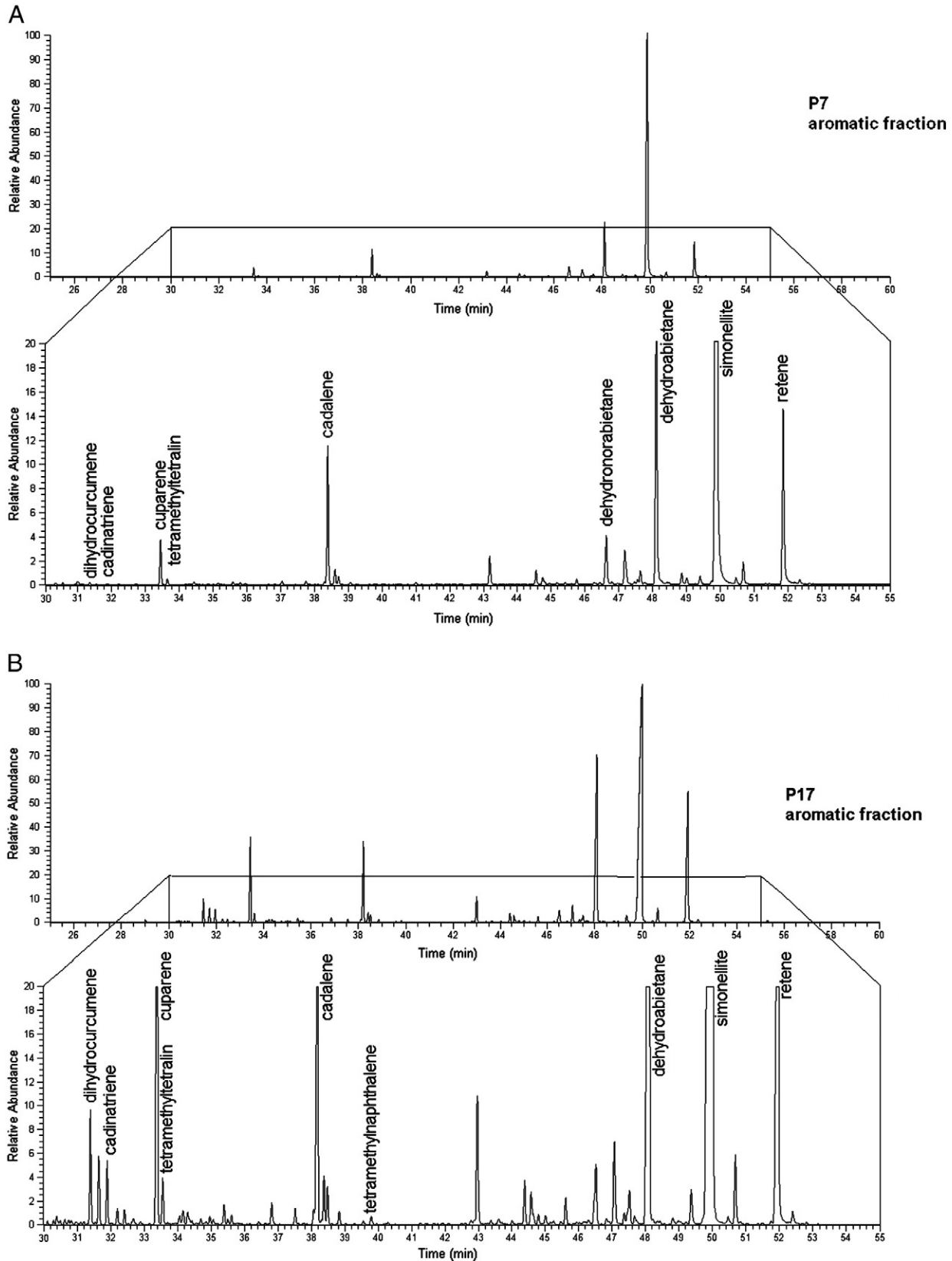


Fig. 8. Typical TIC (Total Ion Current) chromatograms of the aromatic fraction of the sample extracts P7 (A) and P17 (B).

Bechtel et al. (2002, 2003, 2004) and Havelcová et al. (2012) we found a relationship between resinite content and SOM (Fig. 11). Resinite forms round and oval fillings of cellular volumes of tissues and it irregularly fills intercellular spaces. Traces of resinite can be dispersed in cell walls of textinite A and ulminite A.

5.2. Organic compounds

Distribution of *n*-alkanes was similar for all sample extracts: *n*-alkanes with 13 to 32 carbons in the chain have been identified, with a maximum at *n*-C₂₃, and odd-over-even predominance (Fig. 12). The *n*-alkanes are

Table 5
Relative contents of the compounds in the aliphatic hydrocarbon fractions of the stump samples S1–S9 (a) and P1–P23 (b).

a)																							
Compound	S1	S2	S3	S4	S5	S6	S7	S8	S9														
<i>Sesquiterpenoids</i>	0.0	0.0	0.0	0.0	0.0	0.0	2.5	5.8	5.1														
Nordrimane																							
Cedr-8-ene																							
α -cedrane							1.2	3.0	2.3														
Drimane							0.8	2.1	1.3														
Eudesmane							0.5	0.8	1.5														
<i>Diterpenoids</i>	87.1	83.4	84.0	91.6	86.7	89.7	84.3	82.0	82.3														
Norpimarane	11.6	10.1	11.0	10.3	10.6	10.2	11.3	11.3	11.7														
Norabietane	0.6	0.8	0.6	0.7	0.8	0.8	0.9	0.7															
Isopimarane	1.9	2.1	1.9	2.1	2.2	2.1	2.0	2.0	1.9														
Abietane	2.3	2.5	2.4	2.4	2.5	2.4	2.3	2.3	2.2														
α (H)-phyllocladane	70.6	67.8	68.1	76.1	70.5	74.1	67.8	65.7	66.5														
<i>n-alkanes</i>	12.9	16.6	16.0	8.4	13.3	10.3	13.2	12.2	13.0														
b)																							
Compound	P1	P2	P3	P4	P5	P6	P7	P8	P9	P10	P11	P12	P13	P14	P15	P16	P17	P18	P19	P20	P21	P22	P23
<i>Sesquiterpenoids</i>	99.4	99.7	94.8	98.9	97.7	74.0	9.6	93.8	7.5	93.0	87.3	95.3	95.9	98.7	95.9	30.9	73.2	95.8	95.1	94.3	96.8	93.4	30.2
Nordrimane	3.0	1.6	0.1	2.7	3.2	2.3		1.0		0.9	1.7	2.9	3.0	2.3	3.6	4.7	6.4	2.8	4.4	5.7	4.0	2.4	1.2
Cedr-8-ene	1.6	4.6	0.4	2.4	3.3	0.4		0.4		0.5	0.3	1.8	1.0	0.7	1.0	0.5	0.4	1.3	1.1	1.6	1.2	0.9	0.2
α -cedrane	85.5	85.9	84.2	82.3	78.0	62.2	5.5	84.9	4.1	82.2	78.6	64.5	79.5	84.4	86.0	18.5	53.7	86.5	78.6	71.1	84.1	71.7	24.9
Drimane	5.4	3.2	5.4	6.8	8.5	7.0	3.2	4.4	3.0	7.1	8.6	20.8	10.2	8.8	4.5	8.8	12.4	3.6	5.9	13.8	6.6	16.5	5.3
Eudesmane	2.4	1.8	3.5	2.4	2.8	1.5	0.9	2.1	0.5	1.5	1.0	6.9	3.2	2.5	1.2	1.8	1.8	3.4	6.8	2.4	1.5	2.4	1.5
<i>Diterpenoids</i>	0.4	0.2	1.7	0.7	2.0	25.7	89.3	5.9	91.5	6.5	7.7	0.5	1.4	0.5	3.0	48.9	23.1	2.2	2.6	2.4	1.8	4.0	59.9
Norpimarane			0.5		0.1	0.9	2.4		2.4	0.1	1.3	0.4	0.1		0.1	1.0	0.1	0.2	0.1	0.1	0.1	0.1	2.1
Norabietane																							
Isopimarane											0.5					0.1	0.1	0.1	0.1				0.2
Pimarane							1.4		0.8														
Abietane							1.1		1.6						0.2								0.2
α (H)-phyllocladane	0.3	0.2	1.2	0.7	1.9	24.8	84.3	5.9	86.7	6.4	6.3	0.2	1.4	0.5	3.1	53.8	23.6	2.0	2.5	2.3	1.8	4.0	63.6
<i>n-alkanes</i>	0.2	0.1	3.5	0.4	0.4	0.3	1.1	0.3	1.0	0.5	3.4	2.9	1.7	0.5	0.8	12.5	3.2	1.9	2.1	1.4	1.2	1.2	10.4

Significance of italics is the sum of all sesquiterpenoids (diterpenoids, n-alkanes) - main compound groups in the samples.

Table 6
Relative contents of the compounds in the aromatic hydrocarbon fractions of the stump samples S1–S9 (a) and P1–P23 (b).

a)																							
Compound	S1	S2	S3	S4	S5	S6	S7	S8	S9														
<i>Sesquiterpenoids</i>	1.2	2.9	2.5	1.9	4.1	4.6	22.1	29.2	10.7														
Dihydrocurcumene																							
Cadinatriene																							
Cuparene							6.1	11.9	0.4														
Tetramethyltetralin																							
Cadalene	1.2	2.9	2.5	1.9	4.1	4.6	16.1	17.3	10.3														
<i>Diterpenoids</i>	96.7	97.1	97.5	97.2	95.5	95.2	73.1	62.4	89.3														
Dehydrobisorabietane																							
Dehydronorabietanes	4.7	1.8	2.7	3.0	2.6	3.5	8.0	7.9	5.2														
Dehydroabietane	11.1	18.7	18.3	14.4	13.3	13.1	9.8	6.9	14.2														
Simonellite	45.1	67.2	63.5	45.3	50.6	69.1	21.2	12.0	50.0														
Retene	35.8	9.4	13.0	34.5	29.0	9.6	34.1	35.5	19.9														
b)																							
Compound	P1	P2	P3	P4	P5	P6	P7	P8	P9	P10	P11	P12	P13	P14	P15	P16	P17	P18	P19	P20	P21	P22	P23
<i>Sesquiterpenoids</i>	22.9	26.5	13.0	24.0	24.3	16.7	7.8	14.9	8.1	22.2	24.7	11.9	9.8	11.3	15.5	1.8	13.7	27.1	27.6	24.0	10.8	28.4	7.5
Dihydrocurcumene	0.7	0.8	0.1	0.5	0.6	0.6	0.1	0.3	0.1	0.5	1.4	0.7	0.2	0.9	0.4		1.4	0.7	0.1	0.4	0.2	0.9	0.1
Cadinatriene		0.5	0.1	0.3	0.4	0.3		0.1		0.3	0.4	0.1	0.1	0.3	0.3		0.3	0.4	0.4	0.4	0.2	0.5	0.1
Cuparene	6.1	6.5	2.0	6.2	8.5	6.3	1.5	3.6	1.7	7.7	7.3	6.3	2.7	1.5	4.4	0.2	5.8	6.1	2.9	8.6	3.3	10.3	1.6
Tetramethyltetralin	1.8	2.9	0.4	1.4	1.8	1.0	0.2	0.8	0.1	1.1	1.6	2.1	0.6	0.3	0.7	0.1	0.6	2.2	1.1	1.4	0.8	1.2	0.2
Cadalene	14.2	15.7	10.5	15.8	13.0	8.4	6.0	10.1	6.1	12.7	14.0	2.9	6.2	8.3	9.7	1.5	5.7	17.7	23.2	13.2	6.2	15.6	5.5
<i>Diterpenoids</i>	77.1	73.5	87.0	76.0	75.7	83.3	92.2	85.1	91.9	77.8	75.3	88.1	91.3	88.6	84.5	98.2	86.3	72.9	72.4	76.0	89.2	71.6	92n5
Dehydrobisorabietane	0.4	1.5	0.1	0.4	0.6	0.7	0.3	0.7	0.2	0.4	0.5	0.4	0.5	0.6	0.9	0.2	0.5	0.4	0.4	0.2	1.0	0.9	0.4
Dehydronorabietanes	0.4	0.4	0.3	0.4	0.5	1.6	4.0	0.8	1.8	0.3	0.8	0.5	0.4	0.7	0.4	0.2	1.2	0.2	0.3	0.2	0.5	0.5	0.4
Dehydroabietane	0.9	1.8	0.9	1.0	2.3	21.8	11.5	21.2	10.2	14.6	19.3	11.7	10.2	10.0	9.0	7.9	18.2	4.4	2.6	6.9	22.4	26.1	18.3
Simonellite	44.8	36.6	63.5	44.3	43.6	48.7	68.7	50.7	75.0	43.5	32.9	46.5	53.5	34.1	55.0	58.9	53.0	50.5	37.3	51.4	44.1	36.2	57.1
Retene	30.6	33.1	22.2	29.9	28.7	10.6	7.6	11.7	4.7	19.0	21.8	29.0	25.7	43.3	19.3	31.0	13.4	17.4	31.9	17.5	21.2	7.9	16.4

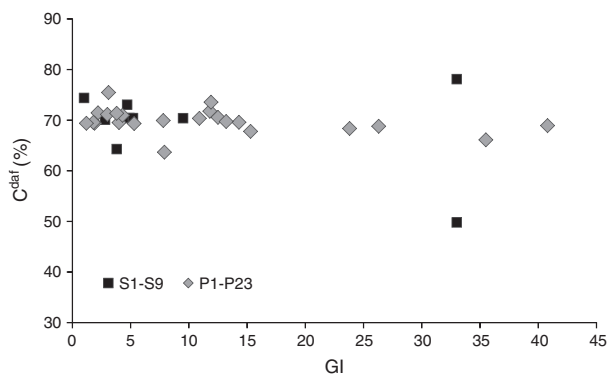


Fig. 9. Relationship between the gelification index (GI) and carbon content (C^{daf}).

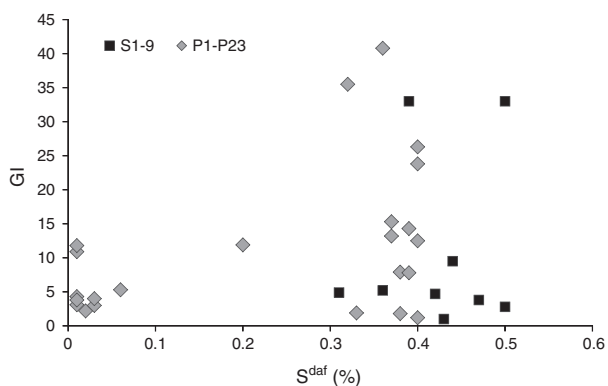


Fig. 10. Relationship between sulphur content (S^{daf}) and gelification index (GI).

characteristic for higher plants, because they originate from their lipids. Carbon Preference Indexes (CPI) (Bray and Evans, 1961) and odd-even predominance (OEP) (Scalan and Smith, 1970) (Table 7) indicate a terrigenous origin of the *n*-alkanes. The lowest values of CPI and OEP have been found in the sample extract P16. The value may have been diminished by geothermal alteration during and after sedimentation or by microbial reworking. The observed *n*-alkane maximum and calculated values (Table 7) correspond to submerged/floating aquatic macrophytes (Ficken et al., 2000; Zheng et al., 2007). Considering the nature and similar storage conditions of the samples, the distribution of *n*-alkanes in the studied samples is associated with a taxon. The similar *n*-alkane distribution in a fossil wood fragment (conifer wood *Protopodocarpoxylon*)

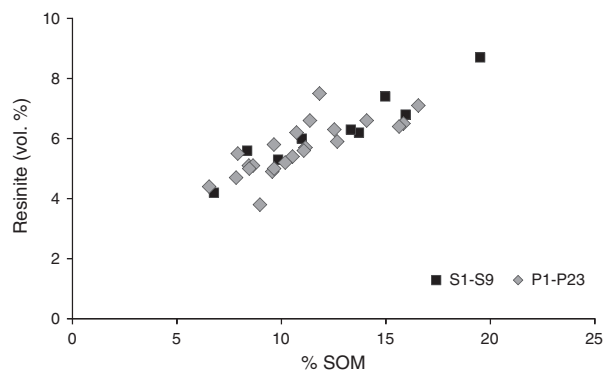


Fig. 11. Relationship between soluble organic matter (SOM) and resinite content.

was identified by Marynowski et al. (2007). Lockheart et al. (2000) and Otto and Simoneit (2001) found that conifer leaves and cones from *Taxodium*, *Sequoia* and *Metasequoia* genera have different distribution of *n*-alkanes compared to other genera.

The results of GC–MS analyses are similar in all wood extracts with regard to terpenoid compounds in the aliphatic and aromatic fractions of the extracts: the most abundant are α -cedrane, $16\alpha(H)$ -phyllocladane, cadalene, dehydroabietane, simonellite, and retene.

The diterpenoid $16\alpha(H)$ -phyllocladane makes up the majority of the substances found in the aliphatic extract of the stump samples S1–S9 (65.7–76.1%), followed by *n*-alkanes (8.4–16.6%) and norpimarane (about 11%). Most of the substances found in the aromatic extract of the stump samples S1–S9 are diterpenoids: dehydroabietane, simonellite and retene, all of which are aromatization products of precursors with the abietane skeleton. These substances constitute more than 90% of the aromatic fraction of the extracts in the S1–S6 samples. Sample extracts S7–S9 contain higher amounts of cuparene and cadalene. Sample extracts from the stumps P1–P23 differ among themselves in proportion of $16\alpha(H)$ -phyllocladane and α -cedrane (Fig. 13). For the stump sample extracts S1–S9 the $16\alpha(H)$ -phyllocladane/ α -cedrane ratio shows minor variations (Fig. 14).

There are other differences in isopimarane, pimaranes (pimarane + norpimarane) and abietanes (abietane + norabietane) distributions in sample extracts P1–P23 (Fig. 15). For the stump sample extracts S1–S9 the variation in relative abundances of these compounds is minor (Fig. 16). The agreement in relationship of the $16\alpha(H)$ -phyllocladane/ α -cedrane ratio and terpenoid occurrences in the stump sample extracts S1–S9 is evident. Among the stump sample extracts P1–P23 the most different are the results in the extracts P7, P9, and P16 having opposite $16\alpha(H)$ -phyllocladane/ α -cedrane ratio.

Hopanoids (hopenes), bacterial markers, were detected only in the stump sample extracts S1–S9, and only in very small quantities, indicating little effect of bacteria on the wood. Non-hopanoid pentacyclic triterpenoids, angiosperm markers, have not been found, and thus no samples can be assigned to angiosperm plants. Identified alkylated aromatic compounds – methyl-naphthalenes, methylbiphenyles, methylphenanthrenes, tetramethyltetralin – (Fig. 12) are degradation products of original terpenoids (Bastow et al., 1998).

Numerous papers have been published on GC–MS application in the study of organic matter of fossil conifers. A summary can be found in a review article by Otto and Wilde (2001), with a list of sesqui-, di- and triterpenoids, which were found in samples and reported between the years 1950 and 1997. The investigation carried by Otto and Wilde (2001) resulted in division of terpenoid substances according to their occurrence: some compounds (e.g., cadinanes, pimaranes) are nonspecific and can be found in all conifer plants, other (e.g., $16\alpha(H)$ -phyllocladane) can be found only in some families of conifer plants, and there are also terpenoids typical for one family only (e.g., cuparenes in Cupressaceae).

Cupressaceae s.l. (Cupressaceae s.str. plus former Taxodiaceae without *Sciadopitys*) are recognized as a single family. This unity is independently supported by similarity of terpenoids. This family can be distinguished by the presence of cuparenes (or other sesquiterpenoids, e.g., widdranes), that occur only in the Cupressaceae s.str.. Pinaceae are distinguished from other conifers because they lack some terpenoids (phenolic abietanes, tetracyclic diterpenoids) and contain some special sesquiterpenoids (longicyclanes, sativanes), diterpenoids (cembranes), and also triterpenoids (serratanes, lanostanes). All other papers published after 2001 have been based on the findings presented in the review by Otto and Wilde (2001): Bechtel et al. (2002), Otto et al. (2002), Hautevelle et al. (2006), Otto et al. (2007), Marynowski et al. (2007), and Bechtel et al. (2007).

Terpenoids and their metamorphic derivatives may have different precursors and that is why tracing of their origin in fossil organic matter is complicated. For example, isopimaranes, pimaranes, and abietanes can come from the labdane-derived copalyl pyrophosphate.

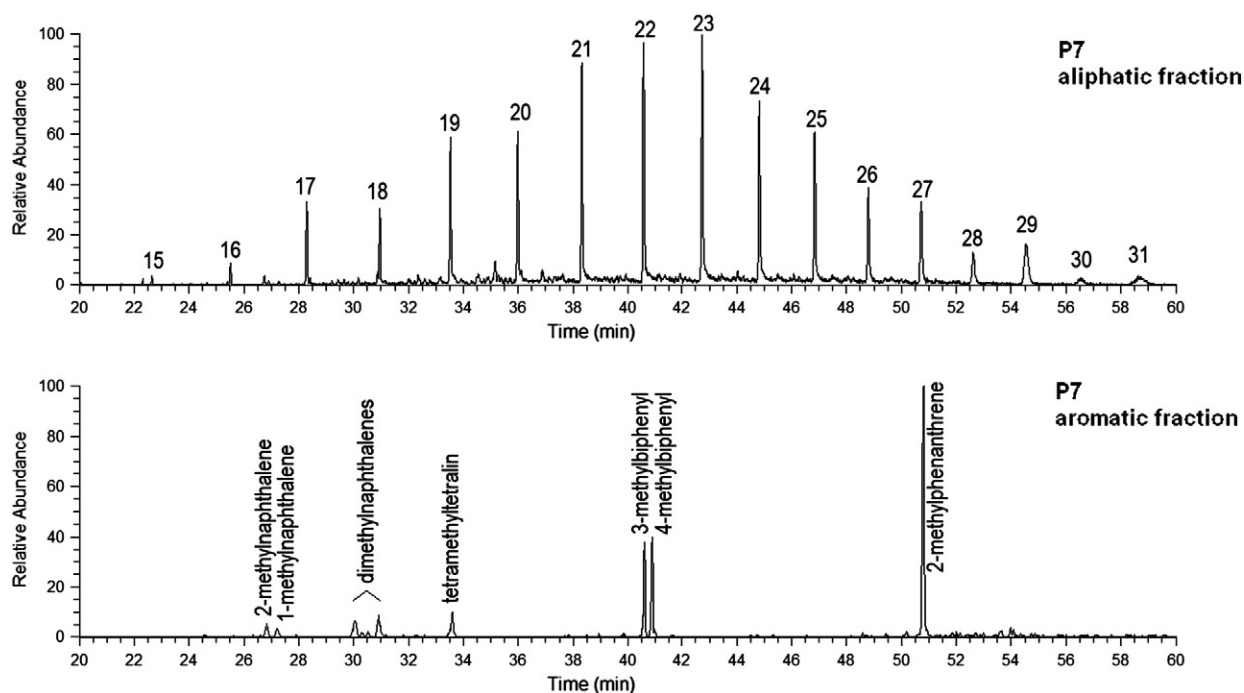


Fig. 12. SIM (Selected Ion Monitoring) chromatograms showing distribution examples of *n*-alkanes (m/z 71) (a) and aromatic compounds (m/z 142, 156, 168, 173, 192) (b). The numbers above peaks indicate carbon numbers of *n*-alkanes.

But they can also come from acids (pimaric, abietic, sandaracopimaric or isopimaric acid), which occur in resins of conifer plants (Otto and Wilde, 2001). The conversion of abietanes then evolves into other compounds – simonellite, retene, and cadalene. But cadalenes may form in an entirely different way, converted from farnesyl pyrophosphate, as well as from α -cedrane or cuparene.

Some of the terpenoid substances found in the studied sample extracts are specific to higher plants and can be assigned to a particular class and family. The occurrence of aliphatic and aromatic biomarkers, arising from native plant materials, depends on conditions during diagenesis of organic matter. Usually, aromatization of plant terpenoids occurs (microbial oxidation, dehydrogenation, and demethylation). If composition of a sample extract is dominated by aliphatic biomarkers, then either the original terpenoid compounds in the plant were special (resistant to degradation) and the storage conditions maintained their status of aliphatics, or the diagenetic conditions were uncommon, reducing primarily production of the aromatic compounds while preserving the aliphatic compounds.

We can assume that the conditions during diagenesis of the plant material were very similar everywhere, and apart from the depositional environment conditions and diagenetic processes also other factors influenced geochemical composition of the material investigated. Differences in the biomarker distribution are related to a conifer family (genus) which original wood has come from. The set of 23 wood fragments is quite representative to exclude random fluctuations in the data. However, among the data from the biomarkers there are at least three samples with more or less intermediate composition.

Staccioli et al. (1993) studied the extracts of the wood of *Taxodioxyton gypsaceum* from Pliocene sediments. The wood revealed the presence of sesqui- and diterpenoid structures, which mainly had cadinane, selinane, and abietane carbon skeletons. The main compounds did not belong to a particular botanical family but also some minor constituents such as α -cedrane were identified. There is a lack of similar data with respect to *Glyptostroboxylon rudolphii*.

According to Otto and Simoneit (2001), cedranes occur only in the family Cupressaceae s.str. and Taxodiaceae, and cuparenes in the family Cupressaceae s.str. and Podocarpaceae of modern wood, and can be used as a characteristic of these conifer plants. Results of the chemical

composition analysis show that the studied samples (or at least those with high content of α -cedrane) belong to one order and appear to be representatives of the family Cupressaceae s.l.

Identical composition of saturated and aromatic hydrocarbons from different parts of stumps and coaly clasts from the surrounding sediment can be considered as an evidence of autochthonous origin of the coaly detritus in the “Stump Horizon”. It can also serve as an evidence of the same way and intensity of diagenetic change of organic matter near one place. But there is also an opposite possibility that the organic matter was altered significantly, and this diagenetic transformation suppressed slight differences and created new ones due to other effects. With respect to the above stated facts it must be said that all studied samples from the stumps S1–S8 and P1–P23 (*Glyptostroboxylon rudolphii* and *Taxodioxyton gypsaceum*) are more coalified and gelified wood fragments, which testifies about humid and warm environment. Such a climate was suitable for most Cupressaceae s.l. with dominantly preserved huminite and relatively high resinite, as it appears in the summary by Kalaitzidis et al. (2004).

6. Conclusion

Results of the study have shown the diversity in maceral and chemical composition among samples of one stump and among samples in a set of 23 tree stumps from the “Stump Horizon” in the Břilina open cast mine in the Most Basin.

Optical microscopy of the fossil stumps has shown plant textures of ulminite and textinite corresponding to botanical structure typical for conifers. Despite an overall bad preservation of anatomical features, SEM has proved all the microscopic structures and enabled a very detailed study of characteristic visual aspects. Stump samples correspond to the species *Glyptostroboxylon rudolphii* and *Taxodioxyton gypsaceum*.

The sample extracts differ in the relative content of the identified compounds. In the sample extracts different ratios of sesquiterpenoids and diterpenoids – α -cedrane and 16 α (H)-phylocladane, respectively – have been found, and different contents of isopimaranes, abietanes, and pimaranes. The samples can be divided into two or three groups (some results are intermediate). The division into two basic groups of samples according to xylotomical parameters does not match the division

Table 7

Values of parameters calculated from the relative n-alkane distribution in the extracts of wood fragments: CPI (Bray and Evans, 1961), P_{aq} (Ficken et al., 2000), P_{wax} (Zheng et al., 2007), OEP 1 and OEP 2 (Scalan and Smith, 1970). S1–S9 (a) and P1–P23 (b).

Sample	CPI	P_{aq}	P_{wax}	OEP1	OEP2
a)					
S1	1.70	0.91	0.22	1.40	1.49
S2	2.21	0.72	0.39	1.20	1.76
S3	1.94	0.81	0.33	1.12	1.67
S4	2.26	0.68	0.40	1.16	1.64
S5	1.98	0.67	0.45	1.08	1.54
S6	2.12	0.65	0.46	1.10	1.58
S7	1.81	0.76	0.37	1.16	1.54
S8	1.99	0.78	0.34	1.09	1.64
S9	2.27	0.75	0.37	1.13	1.80
b)					
P1	2.03	0.93	0.17	1.44	1.48
P2	1.85	0.91	0.20	1.23	1.35
P3	1.52	0.90	0.21	1.19	1.21
P4	1.75	0.91	0.20	1.37	1.29
P5	1.55	0.92	0.19	1.26	1.15
P6	1.99	0.91	0.21	1.42	1.57
P7	2.25	0.82	0.32	1.49	1.94
P8	1.89	0.93	0.19	1.25	1.42
P9	1.64	0.91	0.20	1.19	1.40
P10	2.01	0.95	0.15	1.33	1.45
P11	1.85	0.83	0.29	1.24	1.45
P12	1.57	0.82	0.29	1.12	1.16
P13	1.47	0.79	0.32	1.14	1.12
P14	1.71	0.73	0.38	1.19	1.27
P15	2.08	0.78	0.34	1.35	1.47
P16	0.96	0.64	0.52	0.96	0.89
P17	2.74	0.64	0.45	1.41	1.75
P18	1.71	0.86	0.26	1.24	1.28
P19	1.39	0.78	0.37	1.15	1.18
P20	1.98	0.85	0.25	1.31	1.40
P21	1.80	0.82	0.29	1.30	1.30
P22	2.02	0.75	0.37	1.28	1.51
P23	2.21	0.71	0.41	1.32	1.65

$$CPI = 0.5 * [(C25 + C27 + C29 + C31 + C33) / (C24 + C26 + C28 + C30 + C32) + (C25 + C27 + C29 + C31 + C33) / (C26 + C28 + C30 + C32 + C34)]$$

$$P_{aq} = (C23 + C25) / (C23 + C25 + C29 + C31)$$

$$P_{wax} = (C27 + C29 + C31) / (C23 + C25 + C27 + C29 + C31)$$

$$OEP1 = 1/4 * [(C21 + 6 C23 + C25) / (C22 + C24)]$$

$$OEP2 = 1/4 * [(C25 + 6 C27 + C29) / (C26 + C28)]$$

according to the study of organic matter composition. In the case of Bílina coniferous “Stump horizon”, a GC–MS study of coalified wood has not led to identification of certain genus or species within the family Cupressaceae. The differences in terpenoid composition can be considered as a complex of problems related to diagenetic processes, genus and status of original plant materials that are still subject to further investigation.

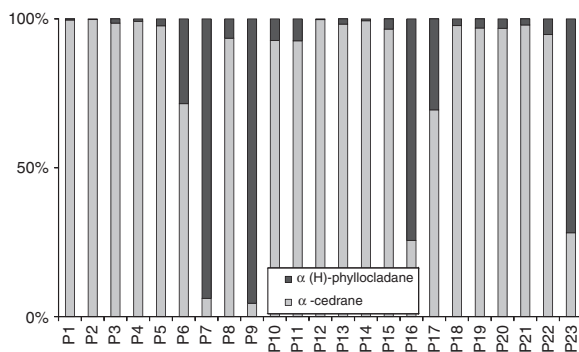


Fig. 13. 16α(H)-Phyllocladane and α-cedrane in samples P1–P23.

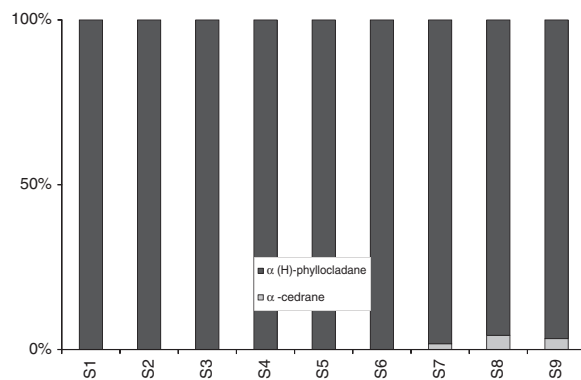


Fig. 14. 16α(H)-Phyllocladane and α-cedrane in samples S1–S9.

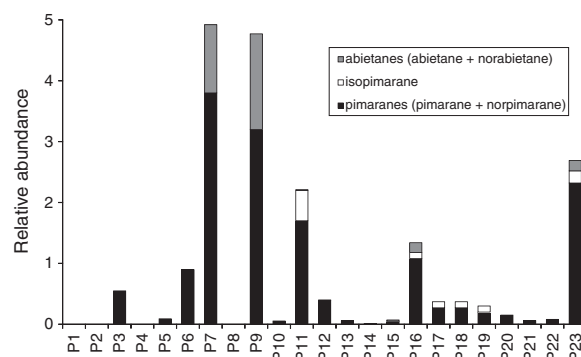


Fig. 15. Relative contents of isopimaranes, pimaranes, and abietanes in samples P1–P23.

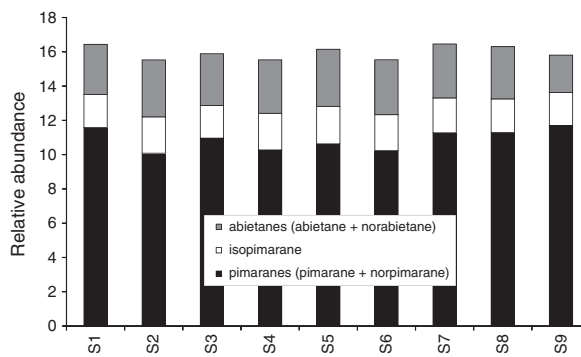


Fig. 16. Relative contents of isopimaranes, pimaranes, and abietanes in samples S1–S9.

Acknowledgements

This study was financially supported by Severočeské doly, a.s., by the project 205/09/1162 of the Czech Science Foundation, and the grant MSM0021620855.

References

- Bastow, T.P., van Aarsen, B.G.K., Alexander, R., Kagi, R.I., 1998. Biodegradation of aromatic land-plant biomarkers in some Australian crude oils. *Organic Geochemistry* 30, 1229–1239.
- Bechtel, A., Sachsenhofer, R.F., Gratzner, R., Lücke, A., Püttmann, W., 2002. Parameters determining the carbon isotopic composition of coal and fossil wood in the Early Miocene Oberdorf lignite seam (Styrian Basin, Austria). *Organic Geochemistry* 33, 1001–1024.
- Bechtel, A., Sachsenhofer, R.F., Markic, M., Gratzner, R., Lücke, A., Püttmann, W., 2003. Paleoenvironmental implications from biomarker and stable isotope investigations on the Pliocene Velenje lignite seam (Slovenia). *Organic Geochemistry* 34, 1277–1298.

- Bechtel, A., Markić, M., Sachsenhofer, R.F., Jelen, B., Gratzner, R., Lücke, A., Püttmann, W., 2004. Paleoenvironment of the upper Oligocene Trbovlje coal seam (Slovenia). *International Journal of Coal Geology* 57, 23–48.
- Bechtel, A., Widera, M., Sachsenhofer, R.F., Gratzner, R., Lücke, A., Woszczyk, M., 2007. Biomarker and stable carbon isotope systematics of fossil wood from the second Lusatian lignite seam of the Lubstów deposit (Poland). *Organic Geochemistry* 38, 1850–1864.
- Bechtel, A., Gratzner, R., Sachsenhofer, R., Gusterhuber, J., Lücke, A., Püttmann, W., 2008. Biomarker and carbon isotope variation in coal and fossil wood of Central Europe through the Cenozoic. *Palaeogeography, Palaeoclimatology, Palaeoecology* 262, 166–175.
- Bray, E.E., Evans, E.D., 1961. Distribution of *n*-paraffins as a clue to recognition of source beds. *Geochimica et Cosmochimica Acta* 22, 2–15.
- Davis, A., Spackman, W., 1964. The role of the cellulose and lignitic components of wood in artificial coalification. *Fuel* 43, 215–224.
- Drobniak, A., Mastalerz, M., 2006. Chemical evolution of Miocene wood: Example from the Belchatow brown coal deposit, central Poland. *International Journal of Coal Geology* 66, 157–178.
- ECE-UN, 1998. International Classification of in Seam Coals. ECE UN, Geneva, p. 41. UN New York.
- Erdei, B., Dolezych, M., Hably, L., 2009. The buried Miocene forest at Bükkábrány, Hungary. *Review of Palaeobotany and Palynology* 155, 69–79.
- Falcon-Lang, H.J., 2005. Intra-tree variability in wood anatomy and its implications for fossil wood systematics and palaeoclimatic studies. *Palaeontology* 48, 171–183.
- Ficken, K.J., Li, B., Swain, D.L., Eglinton, G., 2000. An *n*-alkane proxy for the sedimentary input of submerged/floating freshwater aquatic macrophytes. *Organic Geochemistry* 31, 745–749.
- Figueiral, I., Mosbrugger, V., Rowe, N.P., Ashraf, A.R., Utescher, T., Jones, T.P., 1999. The Miocene peat forming vegetation of northwestern Germany: an analysis of wood remains and comparison with previous palynological interpretations. *Review of Palaeobotany and Palynology* 104, 239–266.
- Figueiral, I., Mosbrugger, V., Rowe, N.P., Utescher, T., Jones, T.P., Von Der Hocht, F., 2002. Role of Charcoal Analysis for Interpreting Vegetation Change and Paleoclimate in the Miocene Rhine Embayment (Germany). *Palaios* 17, 347–365.
- Gryc, V., Sakala, J., 2010. Identification of fossil trunks from Bükkábrány newly installed in the Visitor Centre of the Ipolytarnóc Fossils Nature Reserve (Novohrad – Nógrád Geopark) in Northern Hungary. *Acta Universitatis Agriculturae et Silviculturae Mendeleianae Brunensis* 58, 117–122.
- Hámor-Vidó, M., Hofmann, T., Albert, L., 2010. *In situ* preservation and paleoenvironmental assessment of Taxodiaceae fossil trees in the Bükkábrány open cast mine, Hungary. *International Journal of Coal Geology* 81, 203–210.
- Hatcher, P.G., 1988. Dipolar-dephasing ¹³C NMR studies of decomposed wood and coalified xylem tissue: evidence for chemical structural changes associated with defunctionalization of lignin structural units during coalification. *Energy & Fuels* 2, 48–58.
- Hatcher, P.G., Berger, I.A., Earl, W.L., 1981. Nuclear magnetic resonance studies of ancient buried wood: I Observations on the origin of coal to the brown coal stage. *Organic Geochemistry* 3, 49–55.
- Hauteville, Y., Michels, R., Malartre, F., Trouiller, A., 2006. Vascular plant biomarkers as proxies for paleoflora and paleoclimatic changes at the Dogger/Malm transition of the Paris Basin (France). *Organic Geochemistry* 37, 610–625.
- Havelcová, M., Sýkorová, I., Trejtnarová, H., Šulc, A., 2012. Identification of organic matter in lignite samples from basins in the Czech Republic: Geochemical and petrographic properties in relation to lithotype. *Fuel* 99, 29–142.
- IAWA Committee, 2004. International Association of Wood Anatomists. List of microscopic features for softwood identification. *IAWA Journal* 25, 1–70.
- International Committee for Coal and Organic Petrology (ICCP), 2001. The new inertinite classification (ICCP System 1994). *Fuel* 80, 459–471.
- ISO 7404, 2009. Methods for the petrographic analysis of coal.
- Jeong, E.K., Kim, K., Suzuki, M., Kim, J.W., 2009. Fossil woods from the Lower Coal-bearing Formation of the Janggi group (Early Miocene) in the Pohang Basin, Korea. *Review of Palaeobotany and Palynology* 153, 124–138.
- Kalaitzidis, S., Bouzinos, A., Papazisimou, S., Christanis, K., 2004. A short-term establishment of forest fen habitat during Pliocene lignite formation in the Ptolemais basin, NW Macedonia, Greece. *International Journal of Coal Geology* 57, 246–263.
- Kunzmann, L., Kvaček, Z., Mai, D.H., Walter, H., 2009. The genus *Taxodium* (Cupressaceae) in Paleogene and Neogene of central Europe. *Review of Palaeobotany and Palynology* 153, 153–183.
- Kvaček, Z., 1998. Bílina: a window on Early Miocene marshland environments. *Review of Palaeobotany and Palynology* 101, 111–123.
- Kvaček, Z., Böhme, M., Dvořák, Z., Mach, K., Prokop, J., Rajchl, M., 2004. Early Miocene freshwater and swamp ecosystems of the Most Basin (northern Bohemia) with particular reference to the Bílina Mine section. *Journal of the Czech Geological Society* 49, 1–39 (Prague).
- Lockheart, M.J., van Bergen, P.F., Evershed, R.P., 2000. Chemotaxonomic classification of fossil leaves from the Miocene Clarkia lake deposit, Idaho, USA based on *n*-alkyl lipid distributions and principal component analyses. *Organic Geochemistry* 31, 1223–1246.
- Marynowski, L., Zatoń, M., Simoneit, B.R.T., Otto, A., Jedrysek, M.O., Grelowski, C., Kurkiewicz, S., 2007. Compositions, sources and depositional environments of organic matter from the Middle Jurassic clays of Poland. *Applied Geochemistry* 22, 2456–2485.
- Otto, A., Simoneit, B.R.T., 2001. Chemosystematics and diagenesis of terpenoids in fossil conifer species and sediment from the Eocene Zeitz formation, Saxony, Germany. *Geochimica et Cosmochimica Acta* 65, 3505–3527.
- Otto, A., Wilde, V., 2001. Sesqui-, Di-, and Triterpenoids as Chemosystematic Markers in Extant Conifers – A Review. *The Botanical Review* 67, 141–238.
- Otto, A., Simoneit, B.R., Wilde, V., 2007. Terpenoids as chemosystematic markers in selected fossil and extant species of pine (*Pinus*, Pinaceae). *Botanical Journal of the Linnean Society* 154, 129–140.
- Otto, A., Simoneit, B.R.T., Wilde, V., Kunzmann, L., Püttmann, W., 2002. Terpenoid composition of three fossil resins from Cretaceous and Tertiary conifers. *Review of Palaeobotany and Palynology* 120, 203–215.
- Philp, R.P., 1985. Fossil fuel biomarkers. *Methods in Geochemistry and Geophysics*. Elsevier, New York.
- Rollins, M.S., Cohen, A.D., Bailey, A.M., Durig, J.R., 1991. Organic chemical and petrographic changes induced by early-stage artificial coalification of peats. *Organic Geochemistry* 17, 451–465.
- Russel, N.J., 1984. Gelification of Victorian Tertiary soft brown coal wood I. Relationship between chemical composition and microscopic appearance and variation in the degree of gelification. *International Journal of Coal Geology* 4, 99–118.
- Russel, N.J., Barron, P.F., 1984. Gelification of Victorian tertiary soft brown coal wood II. Changes in chemical structure associated with variation in the degree of gelification. *International Journal of Coal Geology* 4, 119–142.
- Scalan, R.S., Smith, J.E., 1970. An improved measure of the odd-to-even predominance in the normal alkanes of sediment extracts and petroleum. *Geochimica et Cosmochimica Acta* 34, 611–620.
- Staccioli, G., Mellerio, G., Alberti, M.B., 1993. Investigation on terpene-related hydrocarbons from a Pliocene fossil wood. *Holzforschung* 47, 339–342.
- Stach, E., Mackowsky, M.T., Teichmüller, M.J., Taylor, G.H., Chandra, D., Teichmüller, R., 1982. *Stach's Textbook of Coal Petrology*. Gebrüder Borntraeger, Berlin, p. 535.
- Stefanova, M., Markova, K., Marinov, S., Simoneit, B.R.T., 2005. Biomarkers in the fossils from the Miocene-aged Chukurovo lignite, Bulgaria: sesqui- and diterpenoids. *Bulletin of Geosciences* 80, 93–97.
- Stout, S.A., Spackman, W., Boon, J.J., Kistemaker, P.G., Bensley, D.F., 1989. Correlations between the microscopic and chemical changes in wood during peatification and early coalification: a canonical variant study. *International Journal of Coal Geology* 13, 41–64.
- Sweeney, I.J., Chin, K., Hower, J.C., Budd, D.A., Wolfe, D.G., 2009. Fossil wood from the middle Cretaceous Moreno Hill Formation: Unique expressions of wood mineralization and implications for the processes of wood preservation. *International Journal of Coal Geology* 79, 1–17.
- Sykes, R., 1994. A Plant Tissue Origin for Ulminites A and B in Saskatchewan Lignites and Implications for R_p. *Energy & Fuels* 8, 1402–1416.
- Sýkorová, I., Pickel, W., Christanis, K., Wolf, M., Taylor, G.H., Flores, D., 2005. Classification of huminite – ICCP System 1994. *International Journal of Coal Geology* 62, 85–106.
- Taylor, G.H., Teichmüller, M., Davis, A., Diessel, C.F.K., Littke, R., Robert, P., 1998. *Organic Petrology*. Gebrüder Borntraeger, Berlin-Stuttgart, p. 704.
- Teodoridis, V., Sakala, J., 2008. Early Miocene conifer macrofossils from the Most Basin (Czech Republic). *Neues Jahrbuch für Geologie und Paläontologie Abhandlungen* 250, 287–312.
- Vassio, E., Martinetto, E., Dolezych, M., Van Der Burgh, J., 2008. Wood anatomy of the *Glyptostrobus europaeus* “whole-plant” from a Pliocene fossil forest of Italy. *Review of Palaeobotany and Palynology* 151, 81–89.
- Visscher, G.E., Jagels, R., 2003. Separation of *Metasequoia* and *Glyptostrobus* (Cupressaceae) based on wood anatomy. *IAWA Journal* 24, 439–450.
- von der Brelie, G., Wolf, M., 1981. Zur Petrographie und Palynologie Keller und dunkler Schichten in rheinischen Hauptbraunkohlenfö. *Fortschritte in der Geologie von Rheinland und Westfalen* 29, 95–163.
- Wagner, M., 1982. Dopplerization of xylitic coal in the light of petrographic and chemical investigations. *International Journal of Coal Geology* 2, 181–194.
- Witke, K., Götze, J., Rößler, D., Ditrich, M., Marx, G., 2004. Raman and cathodoluminescence spectroscopic investigation on permian fossil wood from Chemnitz – a contribution to the study of the permineralisation process. *Spectrochimica Acta A* 60, 2903–2912.
- Yoon, C.J., Kim, K.W., 2008. Anatomical description of calcified woods from Madagascar and Indonesia by scanning electron microscopy. *Micron* 39, 825–831.
- Zdravkov, A., Bechtel, A., Sachsenhofer, R.F., Kortenski, J., Gratzner, R., 2011. Vegetation differences and diagenetic changes between two Bulgarian lignite deposits – Insights from coal petrology and biomarker composition. *Organic Geochemistry* 42, 237–254.
- Zheng, Y., Zhou, W., Meyers, P.A., Xie, S., 2007. Lipid biomarkers in the Zoigé-Hongyuan peat deposit: Indicators of Holocene climate changes in West China. *Organic Geochemistry* 38, 1927–1940.